PICS International Conference and Exhibition on Instrumentation and Control
PICS-ICEIC 2003
27-29 November 2003, Pan Pacific Hotel, Manila, Philippines

MODELING AND ANALYSIS OF OMNIDIRECTIONAL MOBILE ROBOT TOWARD ISOTROPIC DESIGN

Maung Than Zaw
National University of Singapore
maungtha@comp.nus.edu.sg

Denny Oetomo, Marcelo H Ang Jr.*, Lim Chee Wang[1], Ng Teck Khim
National University of Singapore
[1] Singapore Institute of Manufacturing Technology
* mpeangh@nus.edu.sg

ABSTRACT
Mobile robots with omni-directional motion capabilities are very useful especially in mobile manipulation tasks and tasks in human environment. In this paper, we present the kinematics and dynamic of one class of omni-directional mobile robots that is driven by 2-axis powered caster wheels with non-intersecting axes of motion. Our derivation approach treats the each caster wheel as a serial manipulator and the entire system as a parallel manipulator generated by several serial manipulators with a common end-effector, following the operational space approach and augmented object model introduced by Khatib. The kinematics and dynamic analysis can be used to obtain the optimal design of mobile robot powered by 2-axes caster wheels.

Key Words - isotropy, condition number, operational space, kinetic energy matrix, inertia ellipsoid, mobile robots.

I. INTRODUCTION

Omnidirectional wheeled mobile robots have been an active research area and developed over the past three decades. The advantages of these robots over the legged mobile robots are easy to manufacture, high pay load, high efficiency and they can perform important tasks in environments congested with obstacles and narrow aisles.

There are three types of wheels [1]: the conventional wheels, the omnindirectional wheels, are the wheels that we see everyday, such as those on the cars and trolleys. An omnidirectional wheel is a disk-like wheel with a multitude of conventional wheels mounted on its periphery. The ball wheel is the one that is shaped like a ball. The ball wheel [2, 3] is difficult to implement as it is not possible to place an axel through the ball without sacrificing usable workspace. It is difficult to transmit the power to drive the wheel. There is also the practical need of keeping it robust from collecting dust and dirt from the floor. There has been a lot of effort in the development of omnidirectional wheels [4, 5, 6]. Due to multiple numbers of small rollers on the periphery of the wheel, an undesirable vibration often exists in the motion.

The conventional wheel is probably the simplest and most robust among wheel designs. However, not all conventional wheels are capable of providing omnidirectional motion capability [1, 7, 8]. Chosen in our design was an offset wheel or what is often described as caster wheel [9, 10] (see Fig 1). It has been widely accepted that caster design provides full mobility [11].

The kinematics and dynamics of the mechanism is not new [12]. However, our derivation approach follows the conventional method in treating open chain (serial) and closed chain (parallel) manipulator, by using DH convention, the operational space formulation [13] and the *augmented object model* [14, 15]. The augmented object model was utilized to represent the mobile robot as a system of cooperating manipulators, where each wheel module is modeled a serial manipulator. The objective of the design is to obtain an omnidirectionl mobile robot (with 3 DOF motion capability).

II. KINEMATICS MODELING OF A SINGLE CASTER WHEEL

2.1. Kinematics of Single Wheel

In formulation of kinematics model, we treat the wheel module as a serial link manipulator with two revolute joints and one prismatic joint in instantaneous time. The point of wheel contact with the floor is taken as a revolute joint (σ). This is a passive joint with no position feedback as this is the twist angle between the wheel contact and the floor. With the assumption of wheel rolling without slipping, wheel rolling is treated as a prismatic joint ($r\rho$) since angular velocity and linear velocity of the wheel are linearly related. (where r is radius and ρ is angular velocity of the wheel). The steering joint is the last revolute joint (ϕ) of the system.

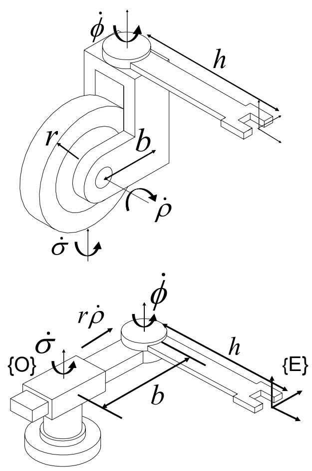

Fig 1. A caster wheel. This design was chosen to provide as omnidirectional motion capability to the mobile platform. Shown in this figure is the instantaneous model of caster wheel

By instantaneous, we mean that the prismatic joint $(r\rho)$ provides an instantaneous linear translation that pushes the end-effector forward with respect to the floor. At the same time, the mechanism has a set length of b (the wheel offset) between thee rotation axes of σ and ϕ. The D-H parameter for the single caster wheel modeled as a serial manipulator is shown in Table 1.

The frame O is an instantaneous frame that is always parallel to the world (absolute) frame, but moves together with the wheel. In other words, it is attached to the contact point between the wheel and the floor.

Joint	α	a	θ	d
1	$-\pi/2$	0	σ	0
2	$\pi/2$	0	0	$r\rho$
3	0	0	ϕ	h

Table 1. D-H parameters of the single wheel

The position of the end-effector with respect to Frame $\{O\}$ is:

$$ {}^{0}p_E = \begin{bmatrix} r\rho C_\sigma + hC_{\sigma+\phi} \\ r\rho S_\sigma + hS_{\sigma+\phi} \\ 0 \end{bmatrix} \tag{1} $$

where $C_\sigma = \cos(\sigma)$, $C_{\sigma+\phi} = \cos(\sigma+\phi)$,
$S_\sigma = \sin(\sigma)$, $S_{\sigma+\phi} = \sin(\sigma+\phi)$

When differentiated, the position vector x will provide the velocity vector of the end-effector, or upon rearranging, the Jacobian matrix and the joint velocity vector. Note that when differentiating $r\rho$ with respect to σ and ϕ, it is taken as the constant value of the offset b, which is the real physical distance. However, when differentiating it respect to ρ, it is taken as variable with respect to time.

Adding the rotational components (the rotational axes of σ and ϕ) into the Jacobian matrix, we obtain:

$$ {}^{0}J_E = \begin{bmatrix} -hS_{\sigma+\phi} - r\rho S_\sigma & rC_\sigma & -hS_{\sigma+\phi} \\ hC_{\sigma+\phi} + r\rho C_\sigma & rS_\sigma & hC_{\sigma+\phi} \\ 1 & 0 & 1 \end{bmatrix} \tag{2} $$

where

$$ \dot{x} = \begin{pmatrix} \dot{x} \\ \dot{y} \\ \dot{\theta} \end{pmatrix} = J \begin{pmatrix} \dot{\sigma} \\ \dot{\rho} \\ \dot{\phi} \end{pmatrix} \tag{3} $$

This is the Jacobian matrix with respect to Frame {O}. Notice that the Jacobian is a function of σ and ϕ. Since σ is not a measurable nor controllable variable, it is desired to have a Jacobian matrix that is not function of σ. This is obtained by expressing the Jacobian with respect to the end-efector frame (Frame {E} in Fig 1)

To do so, the Jacobian is pre-multiplied by a rotational matrix:

$$ {}^{E}J_{E} = {}^{E}R_{0}\, {}^{0}J_{E} \tag{4}$$

where ${}^{E}R_{0}$ is a rotation matrix derived from angle ($\sigma + \phi$).
The resulting Jacobian for a single wheel module with respect to Frame {E} is:

$$ {}^{E}J_{E} = \begin{bmatrix} bS_{\phi} & rC_{\phi} & 0 \\ bC_{\phi} + h & -rS_{\phi} & h \\ 1 & 0 & 1 \end{bmatrix} \tag{5}$$

III. KINEMATICS OF MOBILE BASE

To find the Jacobian matrices of the rest of the wheels, it is only necessary to express them in the common frame (Frame {B}), which is attached to the center of the base:

$$ {}^{B}J_{Ei} = {}^{B}R_{Ei}\, {}^{E}J_{Ei} \tag{6}$$

where *i* denotes the caster wheel of interest, *N* is total number of wheel module in the mobile base and ${}^{B}R_{Ei}$ is the rotation matrix derived from angle β, as shown in Fig 2. This results in the Jacobian of wheel *i* with respect to common Frame {B} at the center of the mobile base:

$$ {}^{B}J_{Ei} = \begin{bmatrix} hS_{\beta_i} + bS_{\beta_i+\phi_i} & rC_{\beta_i+\phi_i} & hS_{\beta_i} \\ hC_{\beta_i} + bC_{\beta_i+\phi_i} & -rS_{\beta_i+\phi_i} & hC_{\beta_i} \\ 1 & 0 & 1 \end{bmatrix} \tag{7}$$

and

$$ {}^{B}J_{Ei}^{-1} = \frac{1}{rb} \begin{bmatrix} rS_{\beta_i+\phi_i} & rC_{\beta_i+\phi_i} & -rhC_{\phi_i} \\ bC_{\beta_i+\phi_i} & -bS_{\beta_i+\phi_i} & bhS_{\phi_i} \\ -rS_{\beta_i+\phi_i} & -rC_{\beta_i+\phi_i} & r(b+hC_{\phi_i}) \end{bmatrix} \tag{8}$$

This derivation yields the same result as the geometric approach found in [12] and [14]. Note that the inverse always exits for $rb \neq 0$.

3.1. Forward Kinematics

In the expression of the Jacobian matrix (Equation 7), we assume that we are able to obtain the joint variable $\dot{\sigma}$ for the purpose of forward kinematics. In the real application, σ is not measurable.

In the inverse kinematics, however, it is possible to remove the σ component (see Equation 8). The inverse of Jacobian matrix without the σ component for any wheel *i* is obtained by simply removing the last row of ${}^{B}J_{i}^{-1}$.

$$ {}^{B}J_{Ei}^{-1} = \frac{1}{rb} \begin{bmatrix} rS_{\beta_i+\phi_i} & rC_{\beta_i+\phi_i} & -rhC_{\phi_i} \\ bC_{\beta_i+\phi_i} & -bS_{\beta_i+\phi_i} & bhS_{\phi_i} \end{bmatrix} \tag{9}$$

which means

$$ \begin{bmatrix} \dot{\rho}_i \\ \dot{\phi}_i \end{bmatrix} = {}^{B}J_{Ei}^{-1} \begin{bmatrix} \dot{x} \\ \dot{y} \\ \dot{\theta} \end{bmatrix} \tag{10}$$

The Jacobian inverse of all the individual wheel modules can be combined to form an augmented Jacobian inverse J_{aug}^{-1}:

$$ \underbrace{\begin{bmatrix} \dot{\phi}_1 \\ \dot{\rho}_1 \\ \dot{\phi}_2 \\ \dot{\rho}_2 \\ \vdots \\ \dot{\phi}_N \\ \dot{\rho}_N \end{bmatrix}}_{\dot{q}_{aug}} = \underbrace{\begin{bmatrix} {}^{E}J_{E1}^{-1} \\ {}^{E}J_{E2}^{-1} \\ \vdots \\ {}^{E}J_{EN}^{-1} \end{bmatrix}}_{J_{aug}^{-1}} . \underbrace{\begin{bmatrix} \dot{x} \\ \dot{y} \\ \dot{\theta} \end{bmatrix}}_{\dot{x}} \tag{11}$$

The forward kinematics can be obtained by solving for $(\dot{x}, \dot{y}, \dot{\theta})^T$ from Equation 11, which represents a 2*N* equations $(N \geq 2)$, for which in general, there may not be a solution. But in this case, the wheel modules are held together by physical constraints:

$$\begin{bmatrix}\dot{x}\\ \dot{y}\\ \dot{\theta}\end{bmatrix} = {}^{E}J_{E1}\begin{bmatrix}\dot{\sigma}_1\\ \dot{\rho}_1\\ \dot{\phi}_1\end{bmatrix} = {}^{E}J_{E2}\begin{bmatrix}\dot{\sigma}_2\\ \dot{\rho}_2\\ \dot{\phi}_2\end{bmatrix} = \cdots = {}^{E}J_{EN}\begin{bmatrix}\dot{\sigma}_N\\ \dot{\rho}_N\\ \dot{\phi}_N\end{bmatrix} \quad (12)$$

therefore an exact solution exist using the left pseudo inverse of J^{-1}_{aug}, i.e.:

$$J_{LPI} = ((J^{-1}_{aug})^T J^{-1}_{aug})^{-1}(J^{-1}_{aug})^T \quad (13)$$

where

$$\begin{bmatrix}\dot{x}\\ \dot{y}\\ \dot{\theta}\end{bmatrix} = J_{LPI}\begin{bmatrix}\dot{\phi}_1\\ \dot{\rho}_1\\ \dot{\phi}_2\\ \dot{\rho}_2\\ \vdots\\ \dot{\phi}_N\\ \dot{\rho}_N\end{bmatrix} \quad (14)$$

Note that J^{-1}_{LPI} always exits for $rb \neq 0$.
When the operation space velocity command vector is obtained from the control law, it can be use immediately used in Equation 11 to produce the joint rate command vector to be sent out to the high level controller for each joint to obtain the desired motion.

IV. KINEMATICS ANALYSIS

The aim of kinematics analysis is to determine the optimal design parameters that exerts, as much as possible, equal effort in joint space to produce any motion in task space. In a serial manipulator, this is often reflect in a manipulator ellipsoid [16] at the end-effector. This is directly related to the singular issues whereby the end-effector loses the ability to move in certain direction (the degenerate direction).

In the case of caster wheel in a mobile base system, singularity is not an issue, always exits, as long as $r \neq 0$ and $b \neq 0$. The exception to this would be when passive joints are include in the system and only 3 joints are actuated to produce motion in 2D plane.

A manipulability ellipsoid, or more appropriately, the *maneuverability ellipsoid*, shows the velocity generated in task space with bounded joint velocities. Please note that it is not appropriate to use the Jacobian matrix in Equation 7, because it still reflects the contribution of the imaginary joint σ. The appropriate analysis should be performed on the J^{-1} matrix without the contribution of σ (from Equation 9) or the Jacobian matrix obtained from Equation 13.

The joint space of a caster wheel, however, only contains two joints: the steer and the drive and it is obvious that when the mobile base diameter is much larger than the wheel radius, then one rotation in steer angle produces a much larger motion than one revolution of the wheel.

V. DYNAMIC MODELING

The caster wheel is treated as a serial link manipulator, each subjected to:

$$A(q)\ddot{q} + b(q,\dot{q}) + g(q) = \tau \quad (15)$$

where τ is the torque to be sent to joint actuators, *A* is the inertia matrix, *b* is vector that contains the Coriolis and Centrifugal effects, and g is the gravitational effect on the joints.

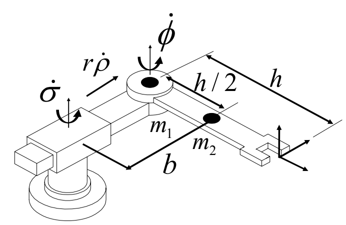

Figure 3: Dynamic model of a wheel module, with three actuators and two canters of mass m_1 and m_2.
The *A* matrix is for individual wheel module is derived by:

$$A = \sum_{i=1}^{3} m_i J^T_{\upsilon_i} J_{\upsilon_i} + J^T_{\omega_i} I_C J_{\omega_i} \quad (16)$$

where the individual caster wheel is modeled as having a center of massed (m_1 and m_2) (Figure

3). The task space kinetic energy matrix Λ_i is obtained for each wheel module i as:

$$\Lambda_i = ({}^B J_i A_i^{-1} {}^B J_i^T)^{-1} \qquad (17)$$

where ${}^B J_i$ is a 3 x 3 matrix of Equation 8.

The combined dynamics of the mobile base at its center, expressed in Frame {B} is obtained by combining the dynamics of all the individual "serial manipulators" reflected at the end-effector (augmented object model [13, 14]):

$$\Lambda_{aug}(q) = \sum_{i=1}^{N} \Lambda_i(q) \qquad (18)$$

VI. DYNAMIC ANALYSIS

The aim of the analysis is to come up with an optimized set of design parameters so that there will be equal in producing motion in all directions. This could be done by analyzing the ellipsoid formed by the eigenvalues and eigenvectors of the Λ_{aug} matrix, which is the inertia of the mobile base in 2D task space [17]. Since the analysis for translational and rotational motion is to be analyzed separately, it is necessary to form separate Λ matrix for translational and rotational motion:

$$\begin{aligned} \Lambda_{\upsilon_i} &= ({}^B J_{\upsilon_i} A_i^{-1} {}^B J_{\upsilon_i}^T)^{-1} \\ \Lambda_{\omega_i} &= ({}^B J_{\omega_i} A_i^{-1} {}^B J_{\omega_i}^T)^{-1} \end{aligned} \qquad (19)$$

where ${}^B J_{\upsilon_i}$ is the top two rows of the Jacobian matrix (for translation motion $\dot{x}$ and $\dot{y}$) and ${}^B J_{\omega_i}$ is the bottom row of the Jacobian matrix for orientation $(\dot{\theta})$.

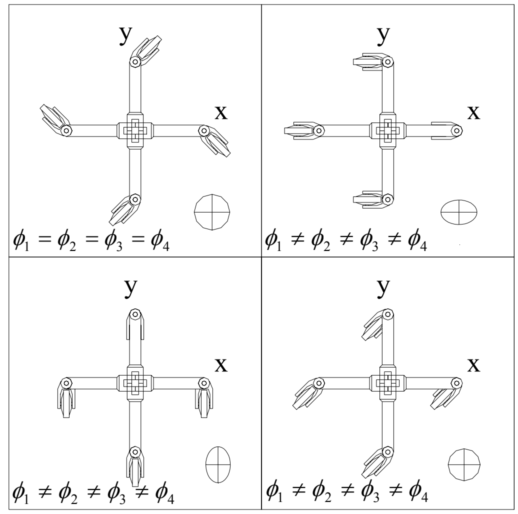

Fig 4: The inertial ellipsoid for translational motion of the combined mobile platform. The minor principal axis of ellipsoid shows the direction that reflects larger inertia in the motion, hence harder to move in those directions.

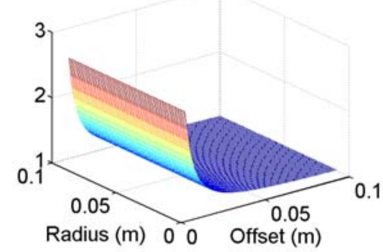

Fig 5: The effect of the design parameters r and b. Offset of the caster wheel plays a major role below a certain threshold value.

An example of the visual representation of the reflected inertia in the 2D planar motion is shown in Fig 4 for translational motion for a mobile base comprised of four sets of wheel module (therefore eight actuated joints).

It is the ideal case when a mobile base is capable of moving in all directions with equal "ease". In this case, the maneuverability ellipsoid will become a circle. Condition number of Λ can be utilized to show the ratio between the major and minor principal of the ellipsoids. A condition number of 1 means that the major and minor principal axes are of the same length.

Figure 5 shows the plot of condition numbers of the combined mobile base (with 4 wheel modules) for various values of radius and offset of the wheel. It is shown that the wheel offset plays a major role below a certain threshold value. The result was produced with example values of h=0.325m (radius of the mobile platform), m_1=1kg for each of the wheels, and m_2=50kg for each of the wheel module.

Our dynamic analysis shows that dynamic isotropic configurations can be achieved when identical powered caster wheels (identical Λ) are distributed in polar symmetric configuration around the centre of the base. Mathematical proof can be shown by making use of the following lemmas and theorem.

Lemma 1. *If A, $B = RAR^T$ (where R is rotation matrix and $A, B \in \Re^{2x2}$) and A+B is symmetric, then*

$$\lambda_k(A) + \lambda_{\min}(B) \le \lambda_k(A+B) \le \lambda_k(A) + \lambda_{\max}(B)$$

where k can either be *max or min.* (20)

And if rotation angle of R is 0, then

$$\lambda_{\max}(A+B) = 2\lambda_{\max}(A) \quad \text{and}$$
$$\lambda_{\min}(A+B) = 2\lambda_{\min}(A)$$

And if rotation angle of R is $\pi/2$, then

$$\lambda_{\max}(A+B) = \lambda_{\min}(A+B) = \lambda_{\max}(A) + \lambda_{\min}(A)$$

The first inequality (20) can be found in Golub and Van Loan [18](pp. 411), and its proof can be found in Wilkinson [19] (pp. 101-2).

Example. If $B = RAR^T$,

$$A = \begin{bmatrix} 5.44 & 1.92 \\ 1.92 & 6.56 \end{bmatrix} \text{ and } R = \begin{bmatrix} \cos\theta & -\sin\theta \\ \sin\theta & \cos\theta \end{bmatrix} \text{then}$$

$\lambda(A)$={4, 8}, $\lambda(A+B)$={8, 16} if $\theta = 0$ and $\lambda(A+B)$={12,12}if $\theta = \pi/2$.

Lemma 2. *If $B = \sum_{i=1}^{N} R_i A R_i^T$ where $N \ge 3$, $A \in \Re^{2x2}$ is symmetric and R is rotation matrix with polar symmetry angle between N, then*

$$\lambda_{\max}(B) = \lambda_{\min}(B) = \frac{N}{2}(\lambda_{\max}(A) + \lambda_{\min}(A))$$

Example. If $B = \sum_{i=1}^{N} R_i A R_i^T$

$$A = \begin{bmatrix} 5.44 & 1.92 \\ 1.92 & 6.56 \end{bmatrix} \text{ and } R_i = \begin{bmatrix} \cos\theta_i & -\sin\theta_i \\ \sin\theta_i & \cos\theta_i \end{bmatrix}$$

for N=3, $\theta_{1,2,3} = 0, 2\pi/3, -2\pi/3$ then $\lambda(A)$ = {4, 8} and $\lambda(B)$ = {18, 18}.

The proofs for Lemmas 1 and 2 are omitted here because of space imitation in this paper. However, the examples given above illustrate the correctness of the lemmas.

Theorem. *If more than two planner manipulators which have two degrees of freedom are augmented with polar symmetry or two of these manipulators are augmented perpendicularly, then the configurations which are made of same corresponding angles are dynamically isotropic.*

Proof:
$$\Lambda_\oplus = \sum_{i=1}^{N} R_i \Lambda_i R_i^T = \sum_{i=1}^{N} R_i J_i^{-T} A J_i^{-1} R_i^T$$

Since being same corresponding angles, all the Jacobian matrices of the wheel are the same.

$$J_1 = J_2 = \cdots = J_N$$

Thus, Λ_i are identical.

$$\Lambda_1 = \Lambda_2 = \cdots = \Lambda_N$$

Using Lemma 1 and 2 for N=2 and $N \ge 3$, then

$$\lambda_{\max}(\Lambda_\oplus) = \lambda_{\min}(\Lambda_\oplus) = \frac{N}{2}(\lambda_{\max}(\Lambda_i(x)) + \lambda_{\min}(\Lambda_i(x))).$$

Therefore, $\Lambda_\oplus$ is isotropic. □

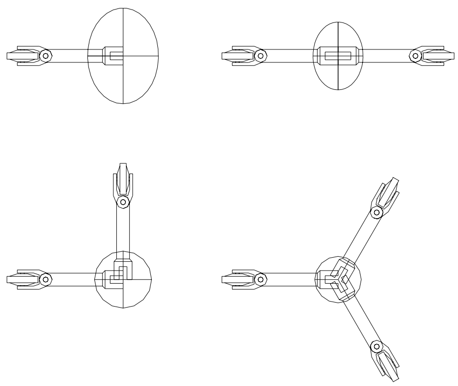

Fig 6: Inertial ellipsoids of wheels in different configurations. The steering angles of all the wheels are assumed to be the same.

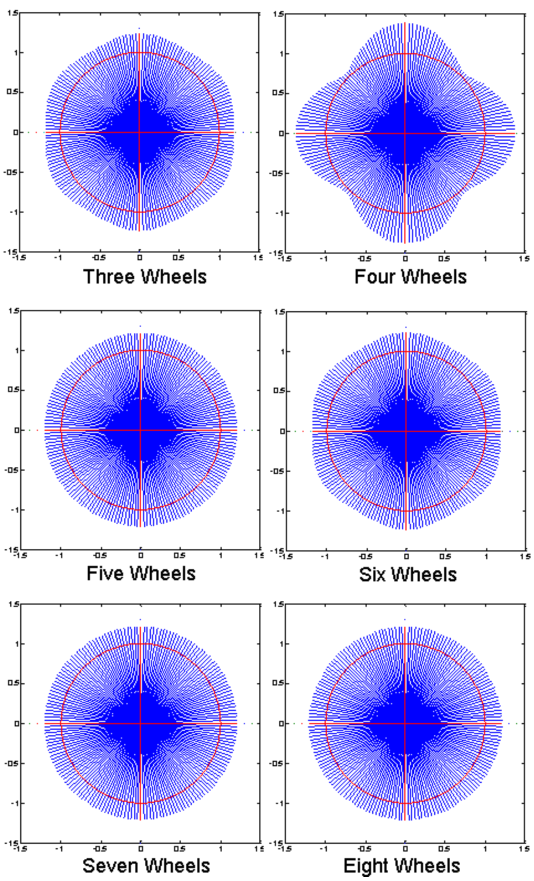

Fig 7: The effect of number of identical wheels on the condition number of Λ as a function of steering angle ϕ for translational motion (therefore all wheels face the same direction). The result is shown for mobile base with six different configurations distributed in polar symmetry.

Fig 6 shows that when two wheels are augmented in 180° the resultant ellipsoid is the same shape as single wheel only different in size. In this figure we assume that all the steering angles of the wheels are the same so that all the Λ are identical. As theorem stated, when two wheels are augmented in 90° or more than two wheels are augmented with polar symmetry the resultant ellipsoid becomes sphere.

Fig 7 shows the condition numbers of Λ in polar plot as a function of steering angle ϕ. The polar angle is the steering angle ϕ and the length is the condition number of Λ. A good design would be one where condition number is close to 1 for all steering angle. The circle with radius 1 represents the condition number of 1. The figure shows dependency of the condition number on steering angle, with the 5 wheels configuration showing least dependency. It is also interesting to note that the four wheel configuration achieves condition number 1 only at ±45°, and ±135°, although the condition number changes more for different steering angles. From isotropy point of view, odd number wheel configurations are better than even number configurations. As can be seen in the Fig, the plot for six wheels is same as three wheels. This plot could be used as a tool for designing a mobile base to achieve isotropic effect with different design parameters.

VII. CONCLUSION

This paper presents the kinematics and dynamics of a mobile robot platform. It models each wheel module as a serial manipulator, where all the serial manipulators have a common operational point, which is attached at the center of the mobile platform. Dynamic analysis was performed to determine the effect of the parameters on the maneuverability of the mobile platform. It was found that an optimal length of offset for the caster wheel was essential so that motion in all direction can be produced with equal effort.

REFERENCES

[1] P. F, Muir and C.P.Neumann, "Kinematic modeling of wheeled mobile robots," *Journal of Robotics Systems*, Vol.4, No.2, pp.281-340, 1987.

[2] S. Ostrovskaya, J.Angles, and R.Spiteri, "Dynamics of a mobile robot with three ball-wheels," *The International Journal of Robotics Research,* Vol. 19, No.3, pp.1-11, 2000.

[3] W. M and H.Asada, "Design and control of ball wheel omnidirectional vehicles," *Proc Intl. Conf Robotics and Automation,* 1995.

[4] L. Ferriere, B. Raucent, and G. Campion, "Design of omnidirectional robot wheels," *Proc. Intl. Conf. on Robotics and Automation,* Vol.4, pp.3664-3670, 1996.

[5] W. La, T. Koogle, D. L. Jaffe, and L. Leifer, "Toward total mobility: an omnidirectional wheelchair," *Proc. 4th RESNA,* pp. 75-77, 1981.

[6] I. Paromtchik and U. Rembold, "Practical approach to motion generation and control for an omnidirectional mobile robot," *Proc. IEEE Intl. Conf Robotics and Automation,* vol. 4, pp. 2790-2795, 1994.

[7] J. Alexander and J. Maddocks, "On the kinematics of wheeled mobile robots," *The International Journal of Robotics Research,* Vol. 8, No. 5, pp15-27, 19889.

[8] S.Ostrovskaya, J. Angeles, and R. Spiteri, "Nonholonomic systems revisited within the framework of analytical mechanisms," *Appl Mech rev,* vol. 51, no. 7, pp 415-433, 1998.

[9] M. Wada and S. Mori, "Holonomic and omnidirectional vehicle with conventional tires," *Proc. IEEE Intl. Conf. Robotics and Automation,* vol. 1, pp. 265-270, 1996.

[10] L. Ferriere, B. Raucent, and A. Fournier, " Design of a mobile robot equipped with off-centered orientable wheels", *Proc. of the Research Workshop of ERNET,* pp. 127-136, 1996.

[11] G. Campion, G. Bastin, and B. D'Andrea-novel, "Structural properties and classification of kinematics and dynamic models of wheeled mobile robots," *IEEE Transactions on Robotics and Automation,* vol. 12, pp. 47-62, February 1996.

[12] B.J. Yi and W.K. Kin, "The kinematics for redundantly actuated omnidirectional mobile robots," *Journal of Robotic Systems,* vol. 12, no. 6, pp. 255-267, 2002.

[13] O.Khatib, "A unified approach for motion and force control of robot manipulators: The operational space formulation," *IEEE J. Robotics and Automation,* vol. RA-3, no. 1, pp. 43-53, 1987.

[14] R. Holmberg, "Design and development of powered-caster holonomic mobile robots," PhD. Dissertation, August 2000. Stanford University.

[15] D. Williams and O. Khatib, "The virtual linkage: A model for internal forces in multi-grasp manipulation," *Pro. IEEE International Conference on Robotics and Automation,* vol. 3, pp. 1025-1030, 1993.

[16] T. Yoshikawa, "Manipulability of robotic mechanisms, " *Intl. J. Robotics Research,* vol. 4, pp. 3-9, Summer 1985.

[17] H. Asada, "A geometrical representation of manipulator dynamics and its application to arm design," *Trans ASME, J. Dyn. Syst., Meas and Control,* vol. 105, pp. 131-135, 1983.

[18] G. Golub and C. Van Loan. "*Matrix Computations*." Johns-Hopkins, Baltimore, second edition, 1989.

[19] J.H. Wilkinson, "*The Algebraic Eigenvalue Problem*," Clarendon Press, Oxford, 1965.